The antigen–antibody unbinding process through steered molecular dynamics of a complex of an Fv fragment and lysozyme

2008 J. Phys.: Condens. Matter 20 255238

(http://iopscience.iop.org/0953-8984/20/25/255238)

IOP PUBLISHING JOURNAL OF PHYSICS: CONDENSED MATTER

J. Phys.: Condens. Matter **20** (2008) 255238 (10pp) doi:10.1088/0953-8984/20/25/255238

The antigen–antibody unbinding process through steered molecular dynamics of a complex of an Fv fragment and lysozyme

Itsuo Hanasaki, Tomoaki Haga and Satoyuki Kawano

Department of Mechanical Science and Bioengineering, Graduate School of Engineering Science, Osaka University, Machikaneyama-cho 1-3, Toyonaka, Osaka 560-8531, Japan

E-mail: hanasaki@me.es.osaka-u.ac.jp and kawano@me.es.osaka-u.ac.jp

Received 13 March 2008, in final form 21 April 2008
Published 22 May 2008
Online at stacks.iop.org/JPhysCM/20/255238

Abstract

We have investigated the antigen–antibody unbinding process using steered molecular dynamics (SMD) simulations. We focus on a complex system consisting of an Fv fragment of an antibody molecule and a lysozyme as an antigen molecule. The Fv fragment consists of a VL and VH chain. The results show that the VH chain is unbound earlier than the VL chain, which is confirmed by the ensemble average of the distance profile obtained from 40 unbinding trajectories. The use of lysozyme as an antigen molecule instead of a small hapten molecule reveals the fact that the induced fit, estimated by the deformation accompanying the unbinding process, is more noticeable for the antigen molecule than for the antibody molecule. The SMD also reveals the non-Gaussian distribution of maximum force necessary for the unbinding process.

1. Introduction

The antigen–antibody reaction is important not only *in vivo* but also *in vitro*, i.e. in clinical medicine and medical engineering. The reactions are used for blood tests by detecting the binding of antigen molecules, so-called tumour markers, to antibody molecules that are immobilized on the inorganic substrate of an artificial device. The antigen–antibody reaction is said to consist of two phases, namely, encounter and recognition. The former is the first step of the binding reaction, and the latter is the completion of the binding by molecular deformation to fit the interface of each molecule. The deformation is called 'induced fit' [1]. The induced fit is not limited to antigen–antibody reactions, but is also related to other biomolecular reactions. In contrast to monoatomic molecular reactions that form diatomic molecules, the antigen–antibody reaction is therefore more complicated. The binding interfaces of each molecule have many atoms that form non-covalent '*bonds*' with those of the other molecule. In this paper, we use the term 'bond' in a broad sense and it includes van der Waals interactions that effectively keep interatomic distances in a certain short range. In fact, much protein–ligand binding consists of many non-covalent bonds.

There are experimental techniques that can be used to obtain the binding energy between a protein and ligand, e.g. isothermal titration calorimetry [2]. Reviews of experimental techniques on protein interactions regarding thermodynamic aspects and general issues are provided in [3] and [4], respectively. Thermodynamic properties such as binding free energies are usually measured in such a way that the individuality of molecules pronounced in the process is rather averaged out. On the other hand, some quantities like the unbinding force can now be measured in a single-molecule manner using atomic force microscopy (AFM) [5–8]. However, information of the structural deformation during the process is not directly obtained. The molecular dynamics (MD) method is often used in such a situation [9]. In particular, steered molecular dynamics (SMD) [10, 11] is useful for the comparison with AFM experiments of the unbinding of the molecular complex. In SMD, the system is steered to undergo a change of state along the reaction coordinate.

The SMD has been applied to several biomolecular systems successfully so far [11] and some of them include the interactions in antigen–antibody systems [12–15]. The entire antibody molecule having a Y-shape is not considered in these studies, but only part of the antibody that binds to the antigen is treated. This is not because of the computational cost but because it is not essential when focusing on the binding after the encounter, and up-to-date AFM experiments also uses the

Fv fragment [16]. As for the antigen molecule, hapten, the smallest kind of molecule that is categorized as an antigen molecule, is exclusively treated. Using a simple specimen leads to a clear understanding without extra factors that can influence the phenomena of interest. This is the positive reason why larger antigen molecules have not been considered. However, it is not enough to fully understand the antigen–antibody reaction. There is a trade-off between making clear remarks by treating simple systems, and obtaining practical information of engineering applications from more realistic systems.

There are some substantial differences between hapten and larger antigen molecules. First, hapten does not deform so much in the course of the binding process. Second, the interaction points and its distribution are locally limited compared to the larger antigen molecules. These differences can sometimes be profound in the characteristics of antigen–antibody reactions. It is therefore insufficient to discuss the properties of a much more complex system using the knowledge of only much simpler systems. The tumour markers are much larger than hapten molecules. Here we investigate the antigen–antibody interaction using a lysozyme molecule as an antigen, which is larger than hapten molecules. We conduct the SMD of the unbinding process between lysozyme and Fv fragment of an antibody, and provide the basic properties observed with an emphasis on the elementary process including deformation. As will be shown later, the deformation of lysozyme is found to be significant.

We focus on obtaining qualitative insight into the antigen–antibody binding phenomena from a non-equilibrium unbinding process by SMD. In principle, the free energy profile can be extracted from SMD using Jarzynski's equality [17], but there is a problem of sampling in some situations [18]. It should be noted that there are several methods that can extract the free energy from MD simulations [19–22]. The MM-PBSA or MM-GBSA method [19] can extract the free energy differences from molecular dynamics (MD), but it does not provide the free energy profile along a reaction coordinate. The adaptive biasing force (ABF) method [20] is a promising alternative if the focus is on the free energy profile.

2. Computational details

In MD, equations of motion are solved for the atoms that constitute the systems of interest. Thus, the collective time evolution of the atomistic systems can be investigated if the potential energy of the system is available. We use the AMBER9 program package [23], and amber ff03 force field [24, 25] for the potential functions and the parameters. The overall potential U_{total} of the standard AMBER force field consists of (covalent) bond, angle, dihedral, van der Waals, and Coulomb potential terms as follows:

$$\begin{aligned} U_{\text{total}} = & \sum_{\text{bonds}} K_r(r - r_{\text{eq}})^2 + \sum_{\text{angles}} K_\theta(\theta - \theta_{\text{eq}})^2 \\ & + \sum_{\text{dihedrals}} \frac{V_n}{2}[1 + \cos(n\phi - \gamma)] \\ & + \sum_{\text{nonbond}} \left(\frac{A_{ij}}{R_{ij}^{12}} - \frac{B_{ij}}{R_{ij}^{6}} \right) + \sum_{\text{nonbond}} \frac{q_i q_j}{\varepsilon R_{ij}}, \end{aligned} \tag{1}$$

where r is the (covalent) bond distance, θ is the angle that is comprised of three neighbouring atoms pertaining to the bonds, ϕ is the dihedral angle comprised of four neighbouring atoms, R_{ij} is the distance between atom i and j, respectively. The K_r, r_{eq}, K_θ, θ_{eq}, V_n, n, γ, A_{ij}, B_{ij}, q_i, q_j and ε are the parameters specified in the force field [24, 25]. We consider a complex system consisting of an Fv fragment of an antibody molecule and a lysozyme molecule. The structure is registered in the protein data bank with PDB code of 1C08 [26]. We simulate the situation where the molecules are in a solvent. The generalized Born (GB) model corresponding to model II in [27] is employed to describe the solvent effect instead of treating it explicitly, without periodic boundary conditions. The cutoff distance of the non-bonded interactions is 12 Å. The maximum distance between the atomic pairs that will be considered in the effective Born radii determination is also 12 Å. The use of explicit water will increase not only the interaction sites to be computed, but also the relaxation time of the molecular configuration. This will also cause the viscous interaction between water that can lead to deformations of the antigen–antibody complex independent of the unbinding phenomena due to the pulling speed that is much faster than AFM experiments. In order to satisfy the same quality in these points as well, the pulling speed should be lower than the case with the GB model, which means a longer time needs to be simulated. Therefore, at the moment it is computationally too expensive to use an explicit water model for the system investigated here.

First, the system is equilibrated through potential energy minimization and subsequent molecular dynamics calculations, and the equilibrium trajectory of the system is sampled for the evaluation of structures and for the use in the SMD as the data of the initial conditions. In order to compare the structure of the bound state with the unbound state, the simulation of not only the Fv–lysozyme complex but also the individual Fv fragment and the lysozyme are conducted separately. The potential energy minimization consists of the first 5000 steps of the steepest descent method and the subsequent 5000 steps of the conjugate gradient method. The equilibration is conducted with a time step of 2 fs using the leap-frog algorithm. The bond lengths pertaining to hydrogen atoms are fixed by the SHAKE algorithm. The temperature of the system is elevated from 0 to 300 K in the first 100 ps. The temperature is controlled by a Langevin thermostat with a collision frequency of 2.0 ps^{-1}. The equilibrium molecular dynamics calculation is conducted with a temperature control at 300 K for 5 ns.

SMD is employed to investigate the unbinding process of the lysozyme and Fv fragment. Although MD is a method suitable for the investigation at the atomistic level of resolution, there are situations where just solving equations of motion is computationally too expensive as the phenomena of interest are rare events. In SMD, an external guiding potential is applied so that the system undergoes the focused phenomena along the prescribed reaction coordinate, and the consequent response of the system is analysed. The principle is analogous to the single-molecule experiments that have become an active area with advances in AFM-related technologies in recent

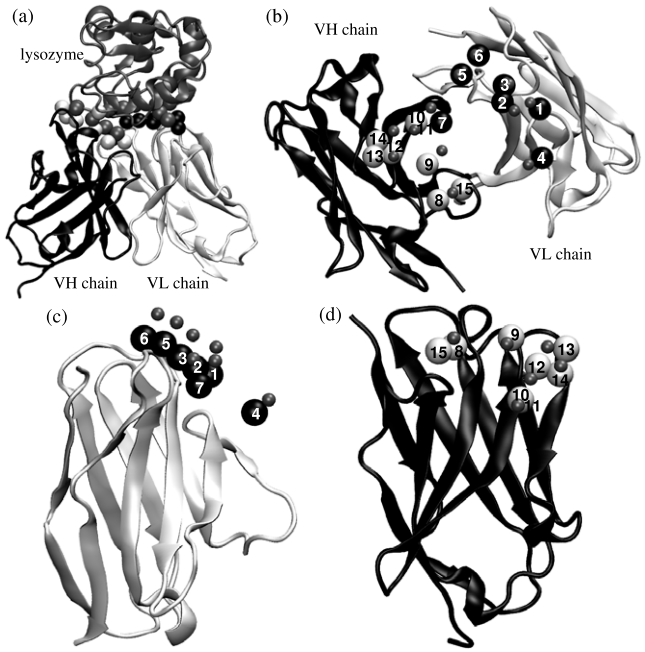

Figure 1. Schematic diagrams of (a) the antigen–antibody complex consisting of the Fv fragment and lysozyme, (b) the 'top' view of the Fv fragment, and the 'side' view of the (c) VL and (d) VH chain. The sphere representation stands for the salt bridges and hydrogen bonds between the Fv and lysozyme. The smaller spheres in (b)–(d) are the atoms of the lysozyme that are shown with the same colour with different size in (a). The numbers written in (b)–(d) correspond to the bond labels in figures 4 and 6.

years [11]. In our case, a harmonic spring with a spring constant of $k_{\mathrm{spring}} = 10$ kcal mol^{-1} Å^{-2} is applied between the lysozyme and Fv fragment and the equilibrium distance is increased steadily during the simulation. More specifically, the complex is pulled apart at a speed of $v = 4$ m s^{-1} starting from the initial configuration that is already equilibrated as mentioned above until it reaches 40 Å from the initial distance. Thus, an SMD simulation takes 1 ns. The pulling speed is faster than those in AFM experiments, but it is limited by the computational cost and is within the range used in many previous works of SMD [28, 12, 13, 29–31]. The dependence of pulling speed on the exerted work is examined later.

The elementary process of the unbinding phenomena is considered to be dependent on the direction of pulling. However, the direction of pulling itself can be defined in numerous ways, and there is no previous report on the detailed study of a deformable antigen unbinding from an antibody as far as we know. Therefore, we do not investigate the effect of the pulling direction comprehensively here. Instead, the pulling condition is assigned so that the direction itself becomes the result rather than the input. Namely, the centres of mass of the major atoms that form intermolecular bonds with each other are specified to be pulled. There are seven non-covalent bonds of the salt bridges and the hydrogen bonds in the VL chain–lysozyme interaction, and eight bonds for the VH chain–lysozyme interaction, which has been reported in [26]. We define the pulling points by the major bonds summarized in table 1 [26]. In this way, no single specific atom is strongly

Table 1. Labelling of major bonds between the Fv fragment and lysozyme. The selection of the bonds is based on [26].

Bond label	Atom of Fv	Atom of lysozyme
1	LAsn-31 Nδ2	His-15 O
2	LAsn-32 Oδ1	Lys-96 Nζ
3	LAsn-32 Nδ2	Gly-15 O
4	LGln-53 Oε1	Asn-93 Nδ2
5	LAsn-92 O	Arg-21 N
6	LAsn-92 Nδ2	Asn-19 O
7	LTyr-96 Oη	Arg-21 Nη1
8	HAsp-32 Oδ1	Lys-97 Nζ
9	HTyr-33 Oη	Lys-97 O
10	HTyr-50 Oη	Arg-21 Nη1
11	HTyr-50 Oη	Ser-100 O
12	HSer-52 Oγ	Asp-101 Oδ1
13	HSer-54 Oγ	Asp-101 Oδ1
14	HSer-56 Oγ	Gly-102 N
15	HAsp-96 Oδ2	Lys-97 Nζ

constrained, and the pulling direction is not assigned directly. What we specify is the sets of the representative points in the lysozyme and Fv fragment that can change the relative positions during the simulations. Nevertheless, they are used to determine the two points necessary to define the actual reaction coordinate, and thus the pulling direction. The system configuration and the correspondence of the labels of the major bonded atoms are schematically shown in figure 1. Visual Molecular Dynamics (VMD) [32] is used for the visualization of the molecules. The molecular secondary structures are displayed by a conventional 'cartoon' representation, and the spheres indicate the positions of the above-mentioned major atoms pertaining to the complex formation.

The simulation protocol in the SMD is essentially the same as that for equilibrium calculations. The temperature control is always applied to the system. Time evolution of the solute dynamics in the GB solvent is faster due to the removal of the solvent molecular degrees of freedom. Therefore, we do not directly focus on the explicitly time-dependent properties, but consider the qualitative trend of unbinding processes concerning molecular deformations. Then, simulation settings that result in many data being sampled in the production run are advantageous for computational efficiency. In addition, the faster equilibration of the system without dissipative interaction with the surrounding solvent makes the fast pulling speed in the SMD more plausible. The main drawback of using GB in this study is that the role of the discrete water molecules on the binding phenomena is not treated explicitly.

3. Results and discussion

The snapshots of one of the unbinding processes by SMD is shown in figure 2. It shows how unbinding of the lysozyme from the VL and the VH chain proceeds. The relative orientation of the Fv fragment and the lysozyme changes as the unbinding proceeds. First, the lysozyme gets unbound from the VH chain, then the bonds between the VL get ruptured. This is just one of the trajectories and inadequate to conclude something only from it, but it is a typical process as we will

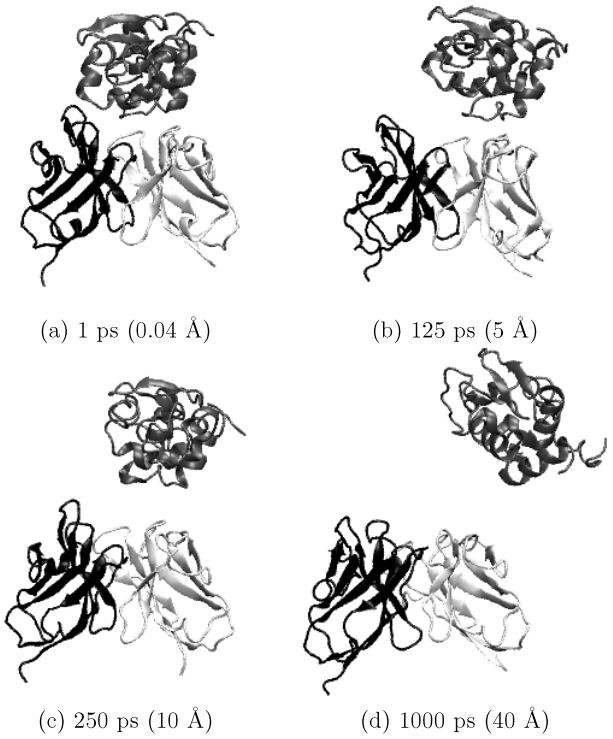

Figure 2. Typical snapshots of the unbinding process by SMD. The white, black, and grey cartoons represent the VL chain, VH chain, and lysozyme molecule, respectively. Values within ( ) represent the target values of the reaction coordinate.

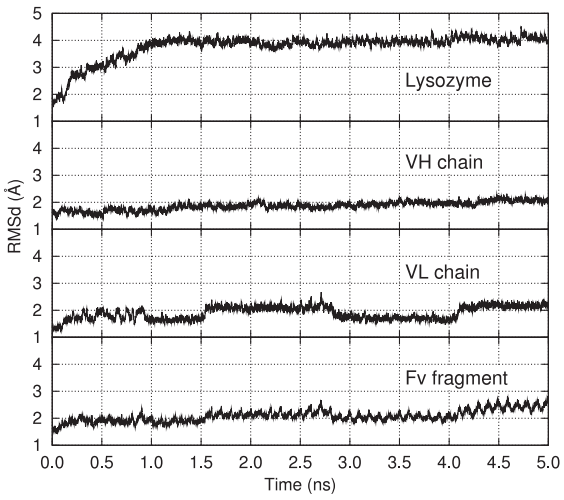

Figure 3. Root mean square deviation of the structures in the Fv–lysozyme complex in equilibrium. The reference structure is that of 1C08.

discuss later. This section consists of two parts: the results and discussion on the equilibrium MD, and those of the SMD.

3.1. Equilibrium molecular dynamics

Before discussing the results of SMD, we first examine the equilibrium properties corresponding to the bound and the unbound state of the Fv fragment and the lysozyme. The root mean square deviation (RMSd) of the VL and VH chains that constitute the Fv fragment, Fv as a whole, and lysozyme molecule are shown in figure 3, which is the result of the equilibrium MD for the Fv–lysozyme complex system. The RMSd in this article refers to the mass-weighted root mean square deviation for all the atoms of the structure to its reference. The reference structure in figure 3 is that of the crystal state. We can see from figure 3 that the lysozyme molecule of the Fv–lysozyme complex in the solvent of the GB model does not remain the same as the crystal structure but deforms for the first 1 ns and reaches an equilibrium state. Therefore, we regard the data after 1 ns as those in equilibrium, and use them for the mean structure evaluation and the initial conditions of the SMD. The structural difference from the experimental value is at least partly due to the fundamental difference of the physical conditions: the experimental value is for the crystal structure, and we simulate the molecules in an aqueous solution. The RMSd of the Fv fragment as a whole shows periodic oscillation. It is not certain whether such an oscillation can be observed in the experiments at the same frequency because the GB solvent model itself does not take into account the dynamic properties that are directly related to the interactions with the surrounding solvent molecules. The Langevin thermostat is a model for the thermal fluctuations of the solvent molecules and the interactions of the solute with them. However, the system behaviour can vary at a quantitative level depending on the collision frequency parameter. Therefore, we focus on the sequential order of the phenomena. The RMSd of the VL and VH chains is relatively small. The RMSd of the VH chain does not noticeably change with time. There are small steps on the RMSd of the VL chain at 1.5, 2.8, and 4.1 ns in figure 3. This suggests that there are two distinctive stable structures in the same environmental condition with only a thermal perturbation on the system. However, the difference of this distinctive but small initial structure does not affect the maximum force or the total work necessary for the unbinding process, as we will see later.

The structural difference of the lysozyme between the bound and the unbound states can be represented by the RMSd of the structure of the bound state from the unbound state, which is different from the one presented in figure 3. The RMSds of the averaged structure of the bound state from the unbound state are 2.0 and 3.1 Å for the Fv fragment and the lysozyme, respectively. Thus, the structural change on the binding or unbinding process is larger for the lysozyme than for the Fv fragment. This RMSd indicates the magnitude of the induced fit in the binding reaction. Therefore, the result suggests that the induced fit occurs more noticeably in the lysozyme than in the Fv fragment. The plausibility of this observation is examined again for the result of SMD.

The distances of the labelled major bonds introduced in the previous section in figure 1 are shown in figure 4. These are the data of equilibrium MD for 5 ns after the short equilibration. None of the data show the transient behaviour indicative of inadequate equilibration. Instead, the bonds labelled 2, 5, 11, and 13 have smaller fluctuations around the mechanical equilibrium distance, which means these bonds are more stable than others. In contrast, the bonds 4, 7, 8,

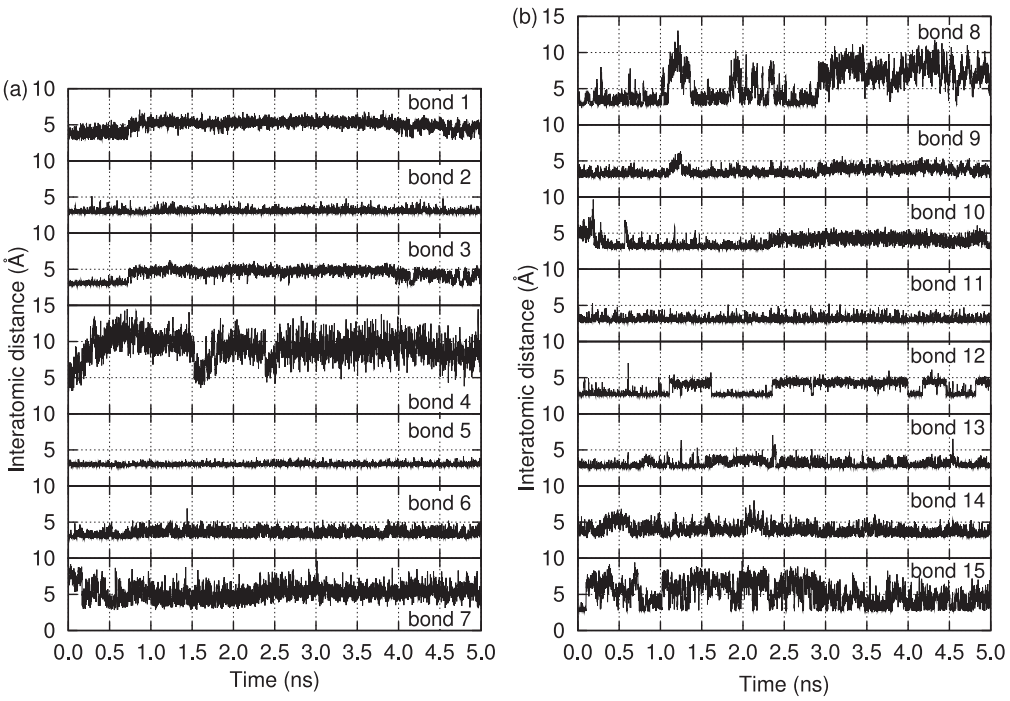

Figure 4. Interatomic distances of the major bonds between the Fv and lysozyme in equilibrium. The bond label numbers in the figure correspond to those labelled on the atoms in figure 1.

and 15 have much larger fluctuations regarding the distances, signifying the unstable nature of the bonds. There is another characteristic bond nature for the bonds 1, 3, 10, and most typically 12. These bonds have multiple stable states under the same equilibrium conditions. Thus, the non-covalent bonds that constitute the antigen–antibody complex of the lysozyme and Fv fragment have not only diversity of robustness, but also multiple states of the binding from a microscopic point of view. It should be noted that the bonds indicated here are not all of the interacting atomic pairs between the lysozyme and Fv fragment that are explicitly described in [26]. Therefore, the bound state of the lysozyme and Fv fragment is the sum of those respective microscopic bond states, and the characteristics of the component bonds may not be observed because they are averaged out after all. It may be said from figure 4 that the bound state of such a complex is not necessarily a microscopically fixed state of the set of the bonds but what could roughly be fixed is the probability distribution of them. This is a characteristic that is at least quantitatively different from that of the complexes consisting of much smaller rigid molecules.

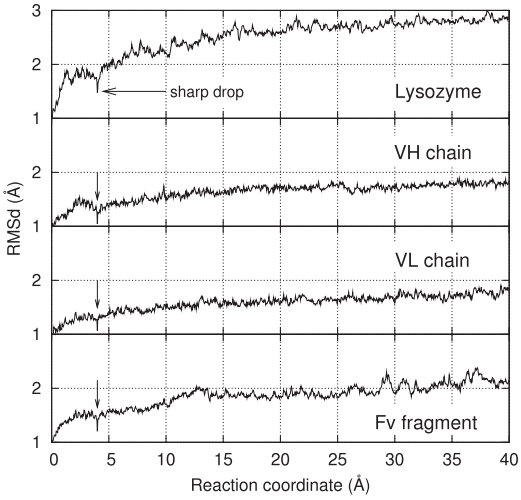

Figure 5. Root mean square deviation of the structure in the SMD as a function of the reaction coordinate. The reference structure is the initial configuration of the SMD. The lines are ensemble averages of the 40 SMD trajectories, respectively. A sharp drop at around 4 Å is observed for every fragment of the system.

3.2. Steered molecular dynamics

Figure 5 shows the ensemble average of the 40 RMSd data for each fragment of the system unbound through the SMD simulation. The reference structure of the RMSd in this figure is the initial configuration of the SMD. The RMSd is plotted as a function of the reaction coordinate but the reaction coordinate here represents the goal distance assigned to the system instead of the actual instantaneous values that the system experiences. The same applies to figures 6, 7, 9, and 11. The difference between the actual instantaneous distance and the targeted equilibrium distance is less than 0.4 Å at the maximum throughout the simulation in the ensemble-averaged data. We thus treat the latter instead of the former as the 'approximate' reaction coordinate except in the discussion of the unbinding length with figure 8. The RMSd of the lysozyme is larger than the Fv fragment as a whole. This is indicative of the induced fit occurring more noticeably for the lysozyme than for the Fv. This characteristic agrees with

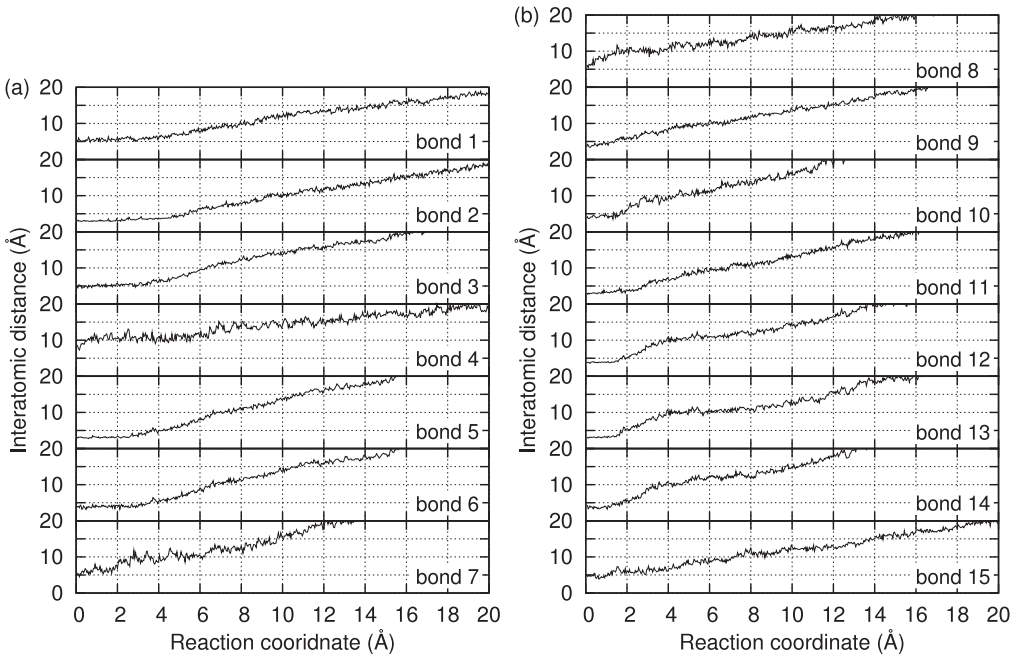

Figure 6. Interatomic distances of the major bonds between the Fv and lysozyme in the SMD. The lines are ensemble averages of the 40 trajectories. The bond label numbers in the figure correspond to those labelled on the atoms in figure 1.

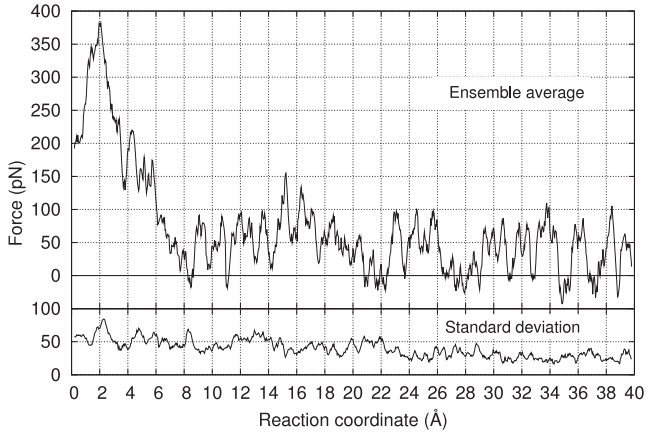

Figure 7. Force profiles in the SMD. The line is an ensemble average of the 40 trajectories that are already moving-averaged with a span of 10 ps at an interval of 1 ps.

the equilibrium investigation of the RMSd discussed above. The increase of the RMSd of the Fv fragment which is larger than those of the VL or the VH chain especially after 10 Å of the unbinding process indicates the change of the relative orientation between the VL and the VH chains as well as the respective deformations of the VL and the VH chains. The RMSd of the VL and VH chains is indistinguishable. Since the magnitude of the RMSd from the initial configuration is not extremely large as a whole, the selection of the pulling points and the pulling speed of 4 m s^{-1} seem to be acceptable. In figure 5, there is a sharp drop of the RMSd at about 4 Å in all of the lysozyme, the VL and VH chain, and the Fv fragment as a whole. The decrease of the RMSd means the partial restoration of the structure to the initial state of the unbinding process. This can be the event where certain critical bonds between the lysozyme and the Fv fragment are effectively broken, which can temporarily diminish the tension between the lysozyme and the Fv fragment. Figure 6 shows the interatomic-distance growth of the 15 bonds mentioned earlier in the SMD simulations. There are several bonds in which the growing rate of the interatomic distances increases at around 4 Å. Specifically, such transitions can be seen in bonds 1, 2, 3, 5, and 6. Thus, the temporary drop of the RMSd in the system at 4 Å is attributed to the bonds breaking between the VL chain and the lysozyme. It is difficult to evaluate whether or to what extent the RMSd of the VL and VH chain is a coupled motion partly because the process is strongly externally driven. However, we can see phenomenologically from figures 5 and 6 that the qualitative change of the interaction originating from effective rupture of the bonds causes deformation of all the constituents of the complex in a similar manner.

The force acting on the reaction coordinate, i.e. the spring between the Fv fragment and the lysozyme through the SMD process is shown in figure 7. Since the original instantaneous force has too much fluctuation to be read, we plot the moving average with a span of 10 ps calculated at an interval of 1 ps. The force profile has the highest peak at 2 Å. Note that this reaction coordinate stands for the difference from the initial length, and not the absolute length itself. It should also be noted that the reaction coordinate mentioned here is not the actual value but the target value, and the actual reaction coordinate where the force reaches the maximum is discussed later. In figure 6, the acceleration of the bond-distance growth at around 2 Å is clearly seen in the bonds 10, 12, 13 whereas it is not observed in the bonds 1–7. This suggests that the unbinding of the VH chain from the lysozyme contributes more than the VL chain, while it is not conclusive only from this

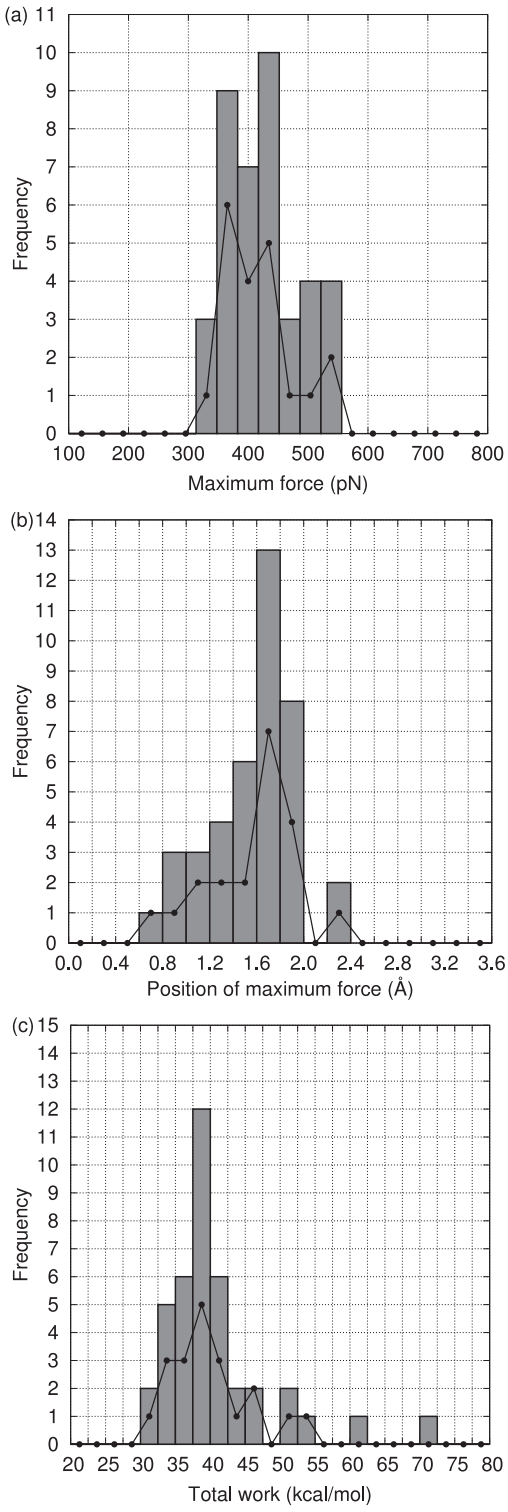

Figure 8. Distribution of (a) the maximum force, (b) the point that the maximum force is realized, and (c) the total work exerted in the SMD. The bars represent the distribution of all the samples, and the filled circles with lines indicate the distribution of the samples taken from those that initially have high RMSd of the VL chain, as shown in figure 3. The force data of the figures are moving-averaged ones, and hence the force fluctuation of short time range is averaged out.

figure. The force has oscillations large enough compared to the standard deviation. This is attributed to the collective motion

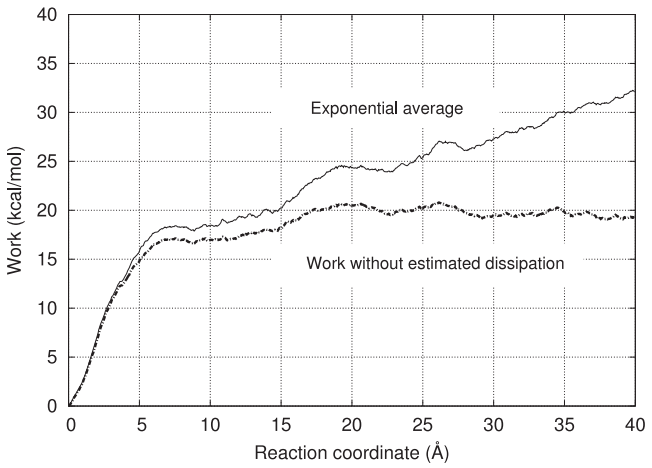

Figure 9. Energy profiles in the SMD simulations. The 'exponential average' is obtained by applying equation (3) to the 40 trajectories of the total work, and 'work without estimated dissipation' is extracted by subtracting the dissipative work estimated from equation (4) from the ensemble average of the total work.

of the system on the molecular level although a quantitative discussion, e.g. on frequency, is difficult due to the model limitation as mentioned earlier.

Histograms of the maximum force and the reaction coordinate that the system takes are shown in figures 8(a) and (b), respectively. The reaction coordinate in this histogram is the actual value that the system takes on that instance. The maximum force is roughly of the order of 400 pN. A recent AFM experiment on the Fv–lysozyme unbinding reports that the unbinding force of a pair of Fv–lysozyme complexes is 50 pN [16]. The much larger unbinding force in the SMD is mainly due to the much higher speed of the unbinding process. The Fv–lysozyme unbinding force in the AFM experiments also increases when the loading rate is increased [16]. In fact, the unbinding force is more than 150 pN when the loading rate is 10^5 pN s^{-1} [16]. The unbinding force of human serum albumin from the antibody is reported to be 244 pN [33], and that of glucagon from the antibody amounts to 256 pN, depending on the pulling speed and pH [34]. Considering the level of the correspondence, it can be said that the pulling speed in the SMD, which is much higher than the experiments, is in the acceptable range. The distribution of the distance from the equilibrium state has a peak in the range of 1.6–1.8 Å. According to the definition in [12], the 'unbinding length' is therefore around 1.7 Å from the equilibrium state. This is around the point where the RMSd of the lysozyme and the Fv fragment ceases the rapid growth, as shown in figure 5. The smooth decrease of frequency with the decreasing distance in figure 8(b) is likely to correspond to the fact that the circumvention of the bond breakages by the deformation of the molecules occurs more easily at the earlier stage of the pulling.

The maximum force is not a simple unimodal distribution. This multimodal distribution reflects the complexity of the unbinding process that consists of the breaking of many bonds accompanied by the deformation of the molecules. Since the distribution is not smooth, it looks like the number of trajectories might not be enough with 40 at first sight.

However, the distributions of the samples taken from those that initially have high RMSd of the VL chain mentioned earlier in figure 3 are the same. The distribution of not only the maximum force but also the point at which the system experiences the maximum force is the same as that of the whole samples. This is the case also for the total work distribution shown in figure 8(c). This implies that the complicated distribution has some physical sense rather than an inadequate number of samples. However, it also suggests that it is non-trivial to determine the dominant factor of the maximum force because the distinctive difference of the initial condition of the VL chain results in the same distribution. The small but distinctive difference in the initial condition of the VL chain structure does not necessarily affect the total energy necessary for the unbinding process.

There is a relation that relates the work W exerted in non-equilibrium processes with the free energy difference ΔF, i.e. the Jarzynski's equality [17];

$$\exp(-\beta \Delta F) = \langle \exp(-\beta W) \rangle, \tag{2}$$

or

$$\Delta F = -\frac{1}{\beta} \ln \langle \exp(-\beta W) \rangle, \tag{3}$$

where $\beta = 1/k_{\mathrm{B}}T$. The line 'exponential average' in figure 9 stands for the work value processed by applying equation (3) for the 40 SMD trajectories. The value increases throughout the SMD process. This is because no trajectory around the region of the free energy profile is sampled due to the fact that the number of samples are limited and that the pulling speed is fast [18]. Jarzynski's equality itself does not depend on the distance from the equilibrium state, i.e. the pulling speed. However, it needs an infinite number of samples to satisfy completely. As can be seen from equation (3), the samples of the low values of work contribute to the average significantly, and those processes rarely occur in systems such as the one treated here.

The pulling-velocity dependence of the total exerted work in SMD is shown in figure 10. The necessary work has not completely converged even at 5 m s^{-1}. However, the dissipative work can be estimated from this pulling-speed dependence as the dissipative work is roughly proportional to the pulling speed. Although there is no surrounding explicit solvent molecule, the dissipative work originates from the coupling with the Langevin thermostat. The linear fit of the total work

$$W_{\mathrm{total}} = w_{\mathrm{d}} v + W_{\mathrm{r}} \tag{4}$$

results in $w_{\mathrm{d}} = 4.31$ kcal s mol^{-1} m^{-1}, $W_{\mathrm{r}} = 28.4$ kcal mol^{-1}, where the W_{r} indicates the lower bound of the reversible work in the unbinding or the binding process. The value is the lower bound because the pulling-speed dependence will disappear at a certain point of the low speed. The work without the dissipative part is also plotted in figure 9, assuming that the dissipative work is generated constantly as the pulling proceeds. The validity of the assumption on pulling-speed dependence can be inferred from the converged, roughly horizontal line after 20 Å, although the converged value in figure 9 indicates that the estimated reversible work is even smaller than the direct linear fit in figure 10. The line has a kink between 5 and 10 Å, which can be interpreted as the point that the major part of the unbinding process completes. The focus of this article is to investigate the process of the unbinding to get some insight into the antigen–antibody reaction. From the derived work without the dissipative component, it is now clearer that the unbinding process completes at around 20 Å. From the viewpoint of energetics, two properties can be found in this figure. The unbinding process consists of two stages, and there is no activation energy where the line has a peak. Such characteristics qualitatively influence the reaction kinetics.

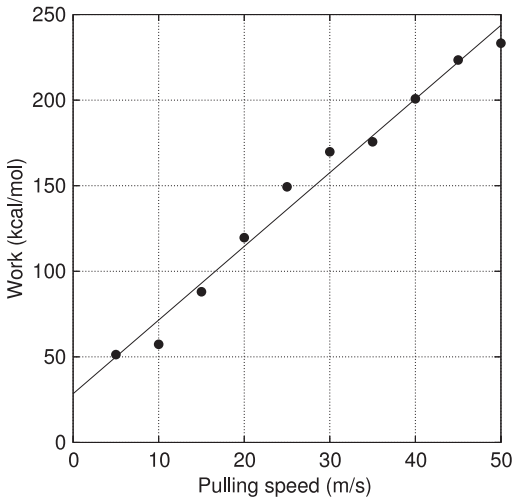

Figure 10. Pulling-velocity dependence of the work in SMD. The points indicated here are results from the single SMD simulations.

To understand the unbinding process on the molecular scale, the change of the distances of the VL chain from the lysozyme and the VH chain from the lysozyme is plotted as a function of the reaction coordinate in figure 11. The lines in the figures are the ensemble averages of the 40 SMD trajectories. The point of the maximum force, i.e. at 2 Å distance from the initial value, or the RMSd drop at 4 Å is not readable from this figure directly, but it can be seen that the VH chain is unbound from the lysozyme earlier than the VL chain; the typical process is schematically illustrated in figure 2. The VL chain remains bound for the first 5 Å pulling process, then starts getting away from the lysozyme. This change of state might be related to the RMSd drop at 4 Å mentioned above. Once pulled away from the lysozyme to some extent, the difference of the distances from the lysozyme does not grow drastically. The growth of the standard deviation moderates at around 10 Å, and it becomes almost constant after 20 Å. This change of state readable from the difference line is similar to the work profile without the dissipative component, which also suggests the validity of the reversible and the dissipative work estimation. The two-stage process seen in the work profile of figure 9 can be related to figure 11. The first 5 Å process of the large work exertion corresponds to the substantial unbinding of the VH chain ahead of the VL chain. The moderate work exertion after that corresponds to the VL chain unbinding as well as the rest of the VH unbinding process. The chain

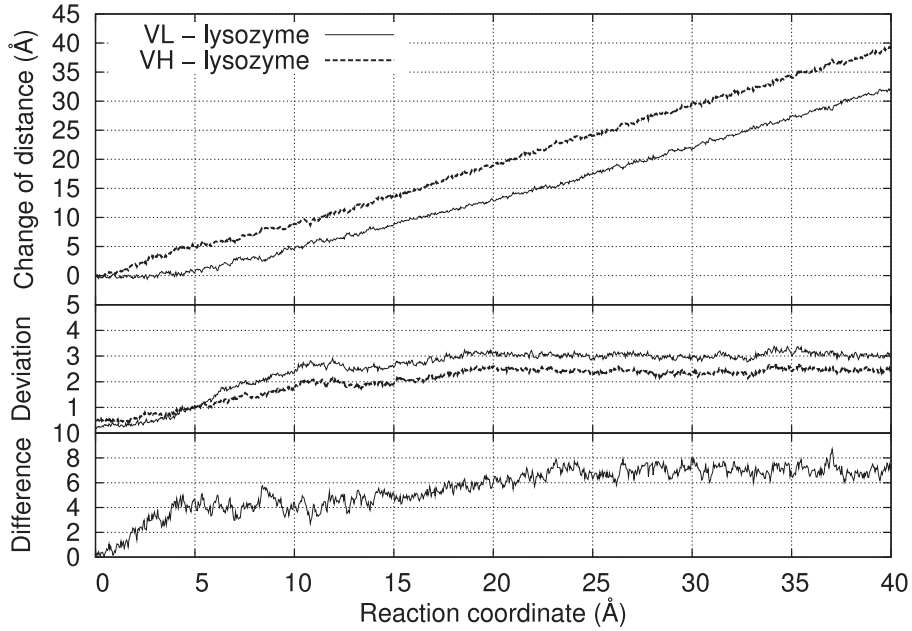

Figure 11. Change of distances of the VL and VH chain from the lysozyme as a function of time. The distances are not those between the centres of mass of each chain but those between the centres of mass of the atoms in each chain that constitutes the major bonds, and the starting points are offset to be zero in the figure.

unbinding order also corresponds to the phenomena that the growth rate of the constituent bond distances between the lysozyme and VH chain typically accelerates at 2 Å followed by the VL chain at 4 Å in figure 6. The sequential order of the VH and VL unbinding that can be observed by the difference of distance growth is obviously larger than the statistical uncertainty measured by standard deviation. Thus, this two-stage process is expected to be observed by the corresponding single-molecule experiments. The question is how to pull the molecules without introducing too much bias into the orientation.

4. Concluding remarks

We have investigated the antigen–antibody unbinding process by the steered molecular dynamics method for the complex of a lysozyme and an Fv fragment. The results indicate that the 'induced fit', a typical process of molecular deformation in an antigen–antibody reaction where the antigen is said to be 'recognized' by the antibody via molecular deformation, is more noticeable for lysozyme, the antigen molecule, than for the Fv fragment, the antibody molecule. The ensemble average of the 40 molecular unbinding processes reveals the tendency that the VH chain of the Fv fragment becomes unbound from the lysozyme earlier than the VL chain. The maximum force distribution is not Gaussian or unimodal but has some complexity of unclear multimodal nature. On the other hand, the difference of the initial structure of the VL chain under the same equilibrium condition is indistinguishable in the distribution of the maximum force or the total necessary work for unbinding.

The determination of the dominant factor of the maximum force is difficult due to the complexity of the system. This is one of the reasons why antigen–antibody unbinding simulations have been limited to systems of small antigen molecules called hapten. However, the use of the deformable antigen molecule reveals the larger deformation of the antigen molecule compared to the antibody molecule. This would have been difficult to find if a hapten molecule had been used because the reaction with the hapten molecule is said to be of lock-and-key type where the antigen molecule does not deform. The strongest drawback or limitation of the present work is that the GB solvent model does not consider the glue effect of water molecules between the antigen and the antibody.

References

[1] Koshland D E Jr 1958 *Proc. Natl Acad. Sci. USA.* **44** 98–104
[2] Perozzo R, Folkers G and Scapozza L 2004 *J. Recept. Signal Transduct.* **24** 1
[3] Holdgate G A and Ward W H J 2005 *Drug Discov. Today* **10** 1543
[4] Piehler J 2005 *Curr. Opin. Struct. Biol.* **15** 4
[5] Clausen-Schaumann H, Seitz M, Krautbauer R and Gaub H E 2000 *Curr. Opin. Chem. Biol.* **4** 524
[6] Willemsen O H, Snel M M E, Cambi A, Greve J, De Grooth B G and Figdor C G 2000 *Biophys. J.* **79** 3267
[7] Allison D, Hinterdorfer P and Han W 2002 *Curr. Opin. Biotechnol.* **13** 47
[8] Hinterdorfer P and Dufrêne Y F 2006 *Nat. Methods* **3** 347
[9] Allen M P and Tildesley D J 1987 *Computer Simulation of Liquids* (Oxford: Clarendon)
[10] Isralewitz B, Gao M and Schulten K 2001 *Curr. Opin. Struct. Biol.* **11** 224–30
[11] Sotomayor M and Schulten K 2007 *Science* **316** 1144
[12] Heymann B and Grubmüller H 1999 *Chem. Phys. Lett.* **303** 1–9
[13] Heymann B and Grubmüller H 2001 *Biophys. J.* **81** 1295–313
[14] Curcio R, Caflisch A and Paci E 2005 *Protein Sci.* **14** 2499–514

[15] Paci E, Caflisch A, Plückthun A and Karplus M 2001 *J. Mol. Biol.* **314** 589–605
[16] Berquand A, Xia N, Castner D G, Clare B H, Abbott N L, Dupres V, Adriaensen Y and Dufrêne Y F 2005 *Langmuir* **21** 5517
[17] Jarzynski C 1997 *Phys. Rev. Lett.* **78** 2690
[18] Park S, Khalili-Araghi F, Tajkhorshid E and Schulten K 2003 *J. Chem. Phys.* **119** 3559–66
[19] Kollman P A, Massova I, Reyes C, Kuhn B, Huo S, Chong L, Lee M, Lee T, Duan Y, Wang W, Donini O, Cieplak P, Srinivasan J, Case D A and Cheatham T E III 2000 *Acc. Chem. Res.* **33** 889
[20] Darve E and Pohorille A 2001 *J. Chem. Phys.* **115** 9169
[21] Rodriguez-Gomez D, Darve E and Pohorille A 2004 *J. Chem. Phys.* **120** 3563
[22] Wang J, Deng Y and Roux B 2006 *Biophys. J.* **91** 2798
[23] Case D A, Darden T A, Cheatham T E III, Simmerling C L, Wang J, Duke R E, Luo R, Merz K M, Pearlman D A, Crawley M, Walker R C, Zhang W, Wang B, Hayik S, Roitberg A, Seabra G, Wong K F, Paesani F, Wu X, Brozell S, Tsui V, Gohlke H, Yang L, Tan C, Mongan J, Hornak V, Cui G, Beroza P, Mathews D H, Schafmeister C, Ross W S and Kollman P A 2006 *AMBER9* (San Francisco, CA: University of California)
[24] Duan Y, Wu C, Chowdhury S, Lee M C, Xiong G, Zhang W, Yang R, Cieplak P, Luo R and Lee T 2003 *J. Comput. Chem.* **24** 1999–2012
[25] Lee M C and Duan Y 2004 *Proteins* **55** 620–34
[26] Kondo H, Shiroishi M, Matsushima M, Tsumoto K and Kumagai I 1999 *J. Biol. Chem.* **274** 27623–31
[27] Onufriev A, Bashford D and Case D A 2004 *Proteins* **55** 383–94
[28] Lu H and Schulten K 1999 *Chem. Phys.* **247** 141
[29] Jensen M Ø, Park S, Tajkhorshid E and Schulten K 2002 *Proc. Natl Acad. Sci. USA* **99** 6731
[30] Park S and Schulten K 2004 *J. Chem. Phys.* **120** 5946
[31] Orzechowski M and Cieplak P 2005 *J. Phys.: Condens. Matter* **17** S1627–40
[32] Humphrey W, Dalke A and Schulten K 1996 *J. Mol. Graph.* **14** 33–8
[33] Hinterdorfer P, Baumgartner W, Gruber H J, Schilcher K and Schindler H 1996 *Proc. Natl Acad. Sci. USA* **93** 3477
[34] Lin S, Wang Y, Huang L, Lin C, Hsu S and Lee C 2007 *Biosens. Bioelectron.* **22** 1013